

5G Multi-Service Field Trials with BF-OFDM

Robin GERZAGUET, Simon BICAÏS, Patrick ROSSON, Jérémy ESTAVOYER, Xavier POPON, David DASSONVILLE, Jean-Baptiste DORÉ, Benoit MISCOPEIN, Manuel PEZZIN, David MIRAS and Dimitri KTÉNAS
CEA-Leti Minatoc, 17 rue des Martyrs, 38054 Grenoble Cedex 9, France
{jean-baptiste.dore}@cea.fr

Abstract—Multi-service transmissions are expected in the upcoming fifth-generation (5G) of cellular networks. These heterogeneous applications lead to many constraints that need to be addressed in a flexible way. We investigate the division of the bandwidth into several subbands, each one having a given physical layer numerology to support a given type of 5G services. This work highlights and demonstrates the possible coexistence of Broadband, Ultra-Reliable Low-Latency and Internet of Things services within the same channel using a flexible waveform. We describe field-test experiments carried out with an implementation of the BF-OFDM (Block-Filtered OFDM) physical layer on custom hardware prototyping boards. Field-trials results confirm the potential of BF-OFDM and the feasibility of the use of mixed numerologies for the next generation of cellular network.

Keywords—Field tests, 5G, BF-OFDM, Prototyping, Baseband, Broadband, IoT, URLLC

I. INTRODUCTION

Although mobile broadband applications will be one of the important drivers of 5G, pushing for higher data rates and capacity than 4G, there is a wide consensus to consider that 5G networks will also have to accommodate various Quality of Service regimes arising with new fields of applications [1] [2]. In particular, IoT (Internet of Things) and ultra-Reliable and Low Latency Communications (URLLC) may represent a true significant digital transformation with tremendous market speculations for 2020. They come with specific challenges on the radio access network design. For instance, IoT requires energy efficiency, long range communications, low cost terminals and the support of a massive number of connected devices. These have been tackled with different approaches, such as narrowband signalling with SigFox [3] or M-ary orthogonal modulations by LoRa [4] and NB-IoT in the context of cellular network [5]. URLLC cover many applications like mission critical communications, vehicular and autonomous driving systems or automated remote control for factories of the future. The corresponding requirements are a reliability of 99.999% of small packet transmissions of 32 bytes with a maximum one-way latency of 1 ms [6][7].

From a physical layer perspective, addressing this wide range of requirements with a unified physical layer in the same system bandwidth is a timely and massive stake which triggers numerous research [8][9]. CP-OFDM (Cyclic Prefix - Orthogonal Frequency Division Multiplexing) [10] stands as the most widespread digital multi-carrier modulation. In particular, its high resilience against multi-path channels with a straightforward implementation has been exploited in many wireless standards (e.g. 4G, WiFi, DVB-T). Still, researchers investigate alternative waveforms, since OFDM suffers from a poor frequency localization and a high PAPR (Peak to Average Power Ratio). Though there is a consensus that 5G is

to rely on multi-carrier scheme, further improvements aspire to release better performances over multi-user and multi-services scenarios with potentially the coexistence of mixed numerologies (different inter carrier spacing, symbol duration, etc).

With regard to the development of 5G orthogonal requirements, many waveforms have been proposed: UFMC (Universal Filtered Multi-Carrier) [11], FBMC (Filter Bank Multi-Carrier) [12], GFDM (Generalized Frequency Division Multiplexing) [13], f-OFDM [9] etc. Thereupon, a novel waveform, entitled BF-OFDM (Block-Filtered OFDM) [14], was recently proposed and proved to be particularly suitable for 5G requirements, i.e. good spectral confinement, flexible structure as well as simple and transparent receiver [15]. Especially, BF-OFDM frequency localization is greatly improved at the price of a slight complexity increase at the transmitter side. Interestingly the BF-OFDM receiver architecture remains identical to the CP-OFDM one. Another advantage of BF-OFDM is to support multi-user asynchronous transmission [14]. Though the waveform was initially designed for mobile broadband wireless access (eMBB), BF-OFDM has been adapted and supports mixed numerology to comply with the URLLC and extended-IoT (eIoT) so that it can be seen as a potential candidate for 5G physical layer.

This paper intends to present field test experiments done with an implementation of the BF-OFDM physical layer on hardware prototyping boards. The frequency band of operation is the 3.5GHz band, for which an experimental license has been granted by ARCEP, the French regulatory body. This experiment is done in an urban-like environment where BF-OFDM is evaluated for representative ranges and propagation conditions covering Line-of-Sight (LOS) and Non Line-of-Sight (NLOS). By collecting quantitative results on SNR and signal demodulation capabilities on various locations, the objective of this study is twofold. It first intends to assess the capability of BF-OFDM to accommodate 5G requirements; secondly it provides feedback from the field on the suitability of the 3.5GHz band in 5G scenarios, in the perspective of its possible designation as a 5G spectrum band.

The paper is organized as follows. Section II presents a recall of the Block-Filtered OFDM and the system model considered for eMBB; the adaption to URLLC and extended-IoT services is also shown. In section III, the proposed testbed is described and results obtained with the proposed system are exposed. A discussion on possible extensions of this work is put across. Eventually, section IV concludes the paper.

II. WAVEFORM AND SYSTEM PARAMETERS

In this section, a recall of the recently proposed BF-OFDM waveform is to be firstly stated. Then, the system parameters for each service is described.

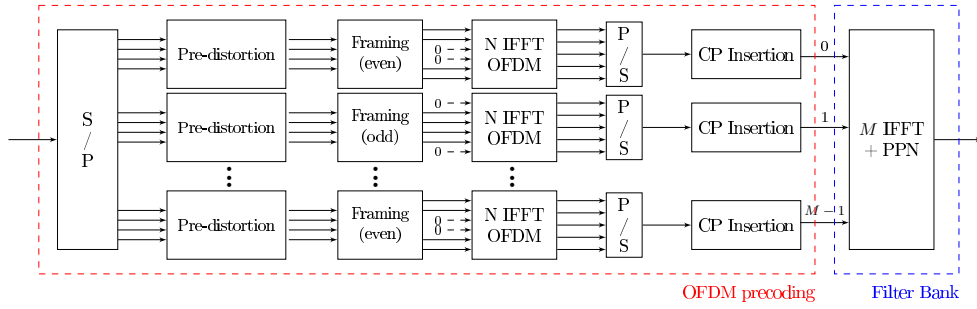


Fig. 1. BF-OFDM transmitter block diagram.

A. BF-OFDM waveform

The transmitter scheme, as described in Figure 1, is composed of M carriers processed by a filter bank stage. Similarly to usual FBMC transmitters, filtering is performed by a PPN (PolyPhase Network) with an overlap and sum operation. Each carrier is the output of an IFFT of N subcarriers. Nonetheless, to maintain subcarrier orthogonality, solely $N/2$ subcarriers are allocated [15]. The mapping of the subcarrier depends on the carrier index parity. Moreover, a pre-distortion stage flattens the transmitted spectrum and allows to avoid match filtering at the receiver [15]. Finally, the cyclic prefix mitigates the ISI (Inter-Symbol Interference) and enables a simple frequency domain equalization.

Inherently, the BF-OFDM receiver is specification transparent, which means that the receiver does not need any knowledge of the filtering applied at the transmitter side. Hence, as depicted in Figure 2, the receiver is analogous to the CP-OFDM one. Moreover, since complex orthogonality is ensured, it is worth mentioning that DFT-precoding for reducing PAPR as well as classical MIMO scheme can be considered with this new waveform for both downlink and uplink. For more details about the concept of BF-OFDM, please see [15] and [14].

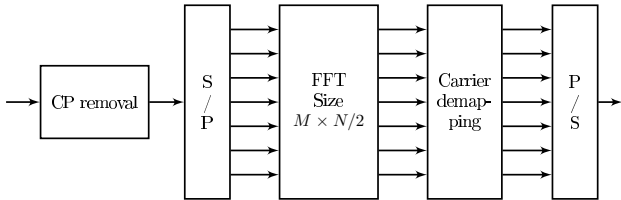


Fig. 2. BF-OFDM receiver block diagram.

B. System parameters

1) *eMBB*: A brief summary of field trials setups and parameters is provided in Table I. A LTE-Like parametrization (180kHz resource block) is considered with scattered pilots, synchronization channels and control channel. The Time Transmission Interval (TTI) is set to 1ms. A control channel sent every ms, indicates the allocation of the users (resource block) as well as the modulation and coding scheme for the transmission. State-of-the-art Forward Error Correction (FEC) scheme is considered, namely turbo coding and rate matching.

TABLE I. EMBB PARAMETERS.

Parameters	Values
Bandwidth	9.72MHz (54 RBs)
TTI	1ms
Sampling Frequency	23.04MHz
Inter-Carrier Spacing	5.625kHz
(M, N, K, N_{CP}) [15]	(128, 64, 4, 4)
Filter	Gaussian 0.33
Modulation	up to 256-QAM
FEC	Turbo-Code 1/3 + Rate Matching

2) *URLLC*: As mentioned previously, URLLC is a service designed to meet delay-sensitivity services with high reliability. Therefore, as depicted in Table II, the duration of the TTI is 0.25ms. A specific frame format has been designed, with a preamble for time and frequency synchronization and also used for channel estimation process. A 16-bytes packet is sent including 3 bytes for control and one byte for CRC. The packet is encoded with a polar code of rate one half. A soft-core polar decoder has been implemented with successive cancellation decoder [16].

TABLE II. URLLC PARAMETERS.

Parameters	Values
Bandwidth	720 kHz
TTI	0.25 ms
Sampling Frequency	23.04MHz
Inter-Carrier Spacing	45kHz
(M, N, K, N_{CP})	(32, 32, 4, 4)
Filter	Dolph Chebychev with stop band attenuation of 90dB
Modulation	QPSK
FEC	Polar code 1/2

3) *eIoT*: The eIoT service waveform has been optimized to present a high robustness over multi-paths channels, a low complexity transceiver with plain integration on an (BF-) OFDM framework and a constant envelope property (null PAPR). The Turbo-FSK scheme [17], fulfills the aforementioned requirements with performances over multi-paths channels similar to OFDM. In detail, it implements a combination of FSK modulation (carrier index modulation), Phase-Shift Keying (PSK) with channel coding, then demodulated by an iterative receiver (turbo principle). For the tests, a 32-bytes packet with a 3-bytes CRC is transmitted at a spectral efficiency of 0.0845. A brief summary of field trial parameters is provided in Table III. The PAPR is lower than 2.6dB, including the preamble and the pilots respectively utilized for time/frequency synchronization and channel estimation. The duration of the transmitted packet is 25ms.

TABLE III. EIoT PARAMETERS.

Parameters	Values
Bandwidth	180kHz
Sampling Frequency	2.88MHz
Inter-Carrier Spacing	5.625kHz
(M, N, K, N_{CP})	(16, 64, 4, 7)
Filter	Gaussian 0.33
Modulation and Coding	Turbo-FSK, 16-PSK

III. FIELD TRIALS

A. Platform and experimental description

The platform developed in this work is flexible. It is composed of a custom digital board and an off-the-shelf radio frequency (RF) transceiver.

The custom digital board is based on the Zynq-045 Xilinx FPGA which integrates a dual Cortex-A9 ARM processor. The block diagram of the Flex system is shown in Figure 3. The base band processing is implemented in the programmable logic while the ARM processor manages non real time algorithms, external components (RF) as well as Media Access Control (MAC) interfaces. A dedicated Linux environment was also built. Ethernet PHY/MAC is provided for easy local area network (LAN) connectivity. The on-board USB On-The-Go (OTG) gives another connectivity option particularly useful to interact with personal computers or other personal devices. The custom digital board has a reduced size ($110 \times 75\text{mm}^2$ see Figure 5).

The RF transceiver board is based on the AD9361 component from Analog Device [18]. It is a high performance, highly integrated radio frequency (RF) Agile Transceiver which combines an RF front end with a flexible mixed-signal baseband section. It supports a dual transmitter and a dual receiver with integrated frequency synthesizers. The AD9361 operates in the 70 MHz to 6 GHz range, covering most licensed and unlicensed bands. Channel bandwidths from less than 200kHz to 56 MHz are supported. The frequency tolerance of the oscillator is approximately ± 20 ppm.

A classical sector antenna from Kathrein supporting dual polarization is used at the transmitter side [19]. The antenna has a 17.5 dBi gain in the frequency range from 3.3 GHz to 3.8 GHz. It covers 65 degree in the azimuth plane while only 6 degree in the elevation plane. A negative mechanical tilt is applied to cover the targeted urban cell. A additional 30dBm Power Amplifier (PA) from Analog Device with filter complemented the transmitter side [20]. At the receiver side a simple omni antenna is connected to the RF transceiver board through pass band filter. It yields a low to medium coverage range.

B. Measurements

For the experimental tests, the transmitter (Tx) antennas and RF units are set on the rooftop of a building, at a height of about 20 meters. Its behavior is similar to a Base Station (BS) (see Figure 4). The receiver, that can be considered as a User Equipment (UE) is mobile. Three configurations are considered: broadband, URLLC and IoT ones. Two scenarios are also assessed: a static scenario and a mobile configuration (30 and 50 km/h).

A single link transmission was considered (DL). The maximum transmit power is 20 dBm. A mixed spectrum allocation was set to emulate a multi-service scenario as depicted in

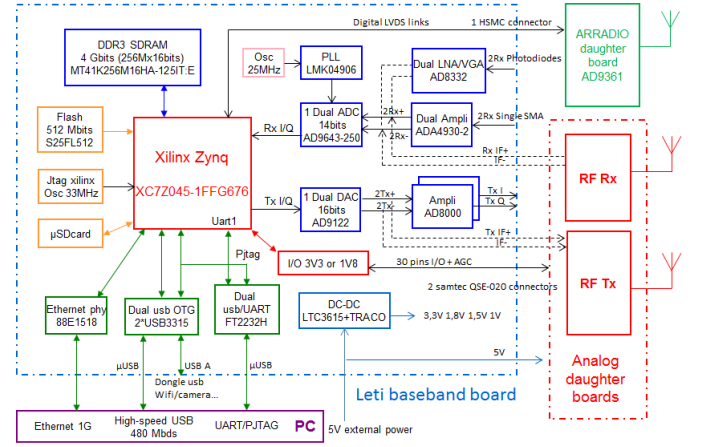


Fig. 3. Flex board architecture.

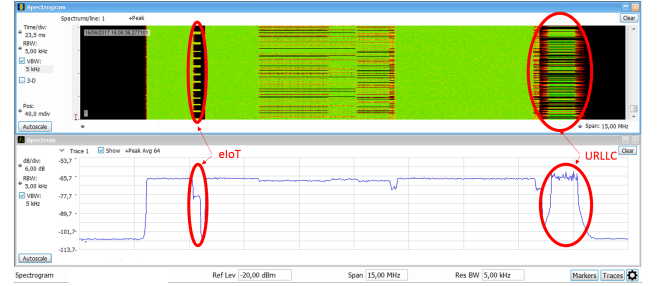


Fig. 4. Snapshot of the frequency allocation acquired by a spectrum analyzer.

Figure 4. The eMBB service is mapped on a 10MHz channel with a 360kHz bandwidth notch for the insertion of the eIoT service. Eventually, at the right edge of the spectrum, the URLLC service is mapped with a 180kHz guard band. All the three services are not synchronized in time as depicted on top of Figure 4.

In the static scenario, the UE is set at a specific location. eMBB service is considered. Different anchors have been defined within the campus as shown in Figure 5. Seven positions have been considered. Some are in Line Of Sight (LOS) such as P1 and P4 and others lie in Non Line of Sight (NLOS) (P2, P3, P5 and P6). The SNR have been evaluated at each locations and are depicted in Figure 6. Results can be summarized as follows:

- P1 is the pure LOS configuration and offers the best performance (Tx to Rx distance 200m).
- P2 is in NLOS as the measurement point is located behind a building (Tx to Rx distance 225m).
- P3 (230m) and P5 (340m) are in NLOS but some reflections from other buildings offer a better performance w.r.t. P2.
- P4 (320m) is in LOS with shadowing due to the trees.
- P6 (390m) and P7 (360m) are in NLOS and are located at the maximal reachable distance.

Figure 8 (top) depicts the channel frequency response and the constellation when the UE is in P4.

Concerning URLLC service, measures in mobility scenario have been assessed. Results are depicted in Figure 7. The SNR

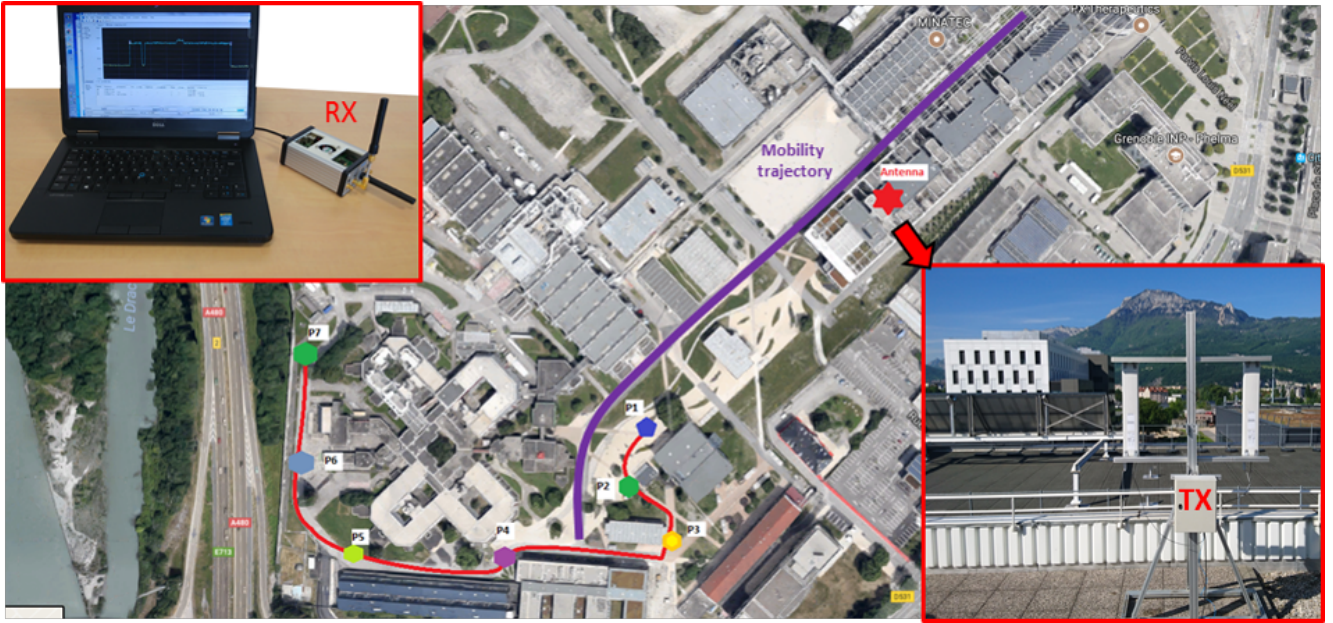


Fig. 5. View of the measurements environment.

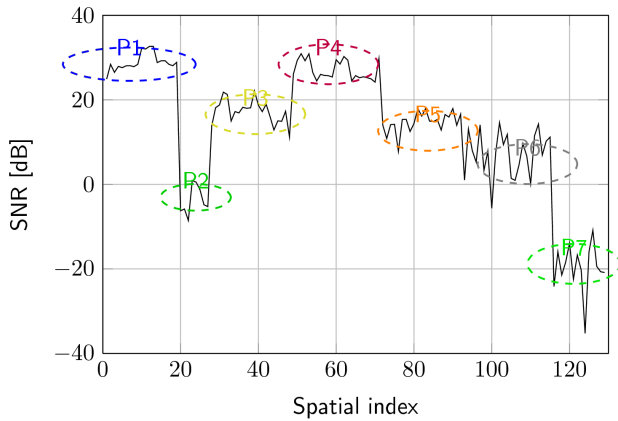


Fig. 6. Variation of the SNR according to the spatial location for eMBB.

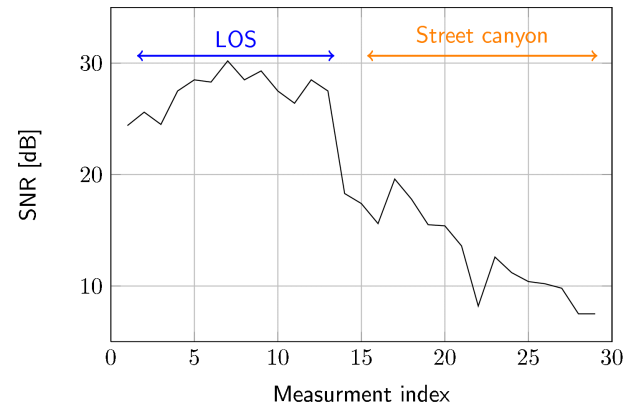


Fig. 7. Variation of the SNR according to the spatial location, URLLC mobility scenario.

estimations were done on the complete trajectory from the LOS to the street canyon induced by the two buildings (20m high) as illustrated Figure 5. The performance loss induced by the NLOS state (street canyon entrance) is clearly visible. Nevertheless the performance is satisfactory on the overall trajectory. Figure 8 depicts the channel frequency response when the UE is in the street canyon. During the test, only a few errors have been encountered.

When it comes to eIoT, the decoding is always successful in fixed condition excepted for the last position (P7). However our investigations have highlighted that the implemented time and frequency synchronization procedure are deficient at very low SNR. Very robust synchronization schemes are required and are currently under design for future measurements.

C. Discussions and perspectives

The consideration of energy constraint waveform for eIoT service has to be discussed. For low throughput scenario, the Turbo-FSK offers a good compromise. Its constant envelope

property points out its performance over classical OFDM and DFT precoding schemes. Moreover, the precoding-FFT algorithm required to reduce PAPR, increases the receiver complexity. Therefore, the use of a new mode based on Turbo-FSK can bridge the gap in the adaptation of a technology for a global cellular IoT. It allows for constant envelope (PA optimization), for integration in an OFDM framework and it enables good performance on typical terrestrial channel model. It makes the technology compatible with both terrestrial and satellite communication. Indeed, a seamless integration of device supporting satellite and terrestrial network is a challenge the proposed solution can fulfill.

In addition to the realized experiment, the set-up will be also considered for two others 5G typical scenarios.

We are currently considering in-band self-backhauling for 5G systems. In-band self-backhauling enables efficient usage of frequency resources. For instance it allows efficient duplexing of radio access network and backhaul. Antenna isolation as well as both analog and digital cancellers enables reuse of

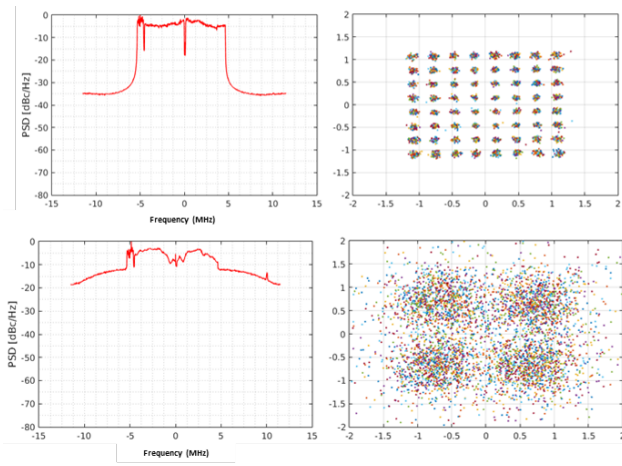


Fig. 8. Snapshot of the measure realized. Top: eMBB LOS. Bottom URLLC NLOS.

the same resources for backhaul and network services. Our initial results [21] are currently being validated in the same framework of experimental measurements in 3.5GHz band.

We are also addressing the concept of extended Dynamic Spectrum Access (eDSA) for which the inter-cell interference in ultra-dense networks is managed thanks to the aggregation of heterogeneous spectrum chunks where user and control traffic can be dynamically steered [22]. A Time Division Duplexing (TDD) MAC protocol based on listen-before-talk and assuming a filtered multi-carrier modulation like BF-OFDM has been designed to operate in the unlicensed 5GHz band. It particularly exploits the tolerance to non-synchronous transmission when receiving multiple signals in the allocation of uplink resource. This MAC protocol will be tested on this field test deployment in order to demonstrate its ability to facilitate the coexistence with other systems, by both fine-tuning Listen-Before-Talk (LBT) thresholds and implementing smart channel re-selection procedures.

IV. CONCLUSION

Multi-service transmissions are expected in the upcoming fifth-generation (5G) of cellular networks. These heterogeneous applications lead to many constraints that need to be addressed in a flexible way. We demonstrate the benefits of considering BF-OFDM in such a scenario. The non-synchronous coexistence of three services, namely eMBB, URLLC and eIoT have been demonstrated. The complete set-up has been presented and initial performance has been assessed. As expected by numerical simulations, field trial results confirm the feasibility of the use of mixed numerologies for the next generation of cellular network. The presented results are a first milestone, and a new measure campaign is planned to consolidate the initial results.

V. ACKNOWLEDGMENT

The research leading to these results received funding from the European Commission H2020 program under grant agreement number 671705 (SPEED-5G project) and number 723247 (5G-Champion project). It also received funds from the French National Research Agency (ANR) within the frame of the DUPLEX project.

REFERENCES

- [1] N. Alliance, "5G White Paper." [Online]. Available: <https://www.ngmn.org/5g-white-paper.html>
- [2] 5GPPP, "5G Architecture." [Online]. Available: <https://5g-ppp.eu/white-papers/>
- [3] SigFox. Sigfox, the worlds leading Internet of things (IoT) connectivity service. [Online]. Available: <https://www.sigfox.com/en>
- [4] L. Alliance. LoRa Alliance, Wide Area Networks for IoT. [Online]. Available: <https://www.lora-alliance.org/>
- [5] R. Ratasuk, N. Mangalvedhe, Y. Zhang, M. Robert, and J. P. Koskinen, "Overview of narrowband IoT in LTE Rel-13," in *2016 IEEE Conference on Standards for Communications and Networking (CSCN)*, Oct 2016, pp. 1–7.
- [6] "TR 38.913 - Study on scenarios and requirements for next generation access technologies - Release 14," October 2016.
- [7] S. Eldessoki, B. Holfeld, and D. Wieruch, "Impact of Waveforms on Coexistence of Mixed Numerologies in 5G URLLC Networks," in *WSA 2017; 21th International ITG Workshop on Smart Antennas*, March 2017, pp. 1–6.
- [8] R. Gerzaguat, N. Bartzoudis, L. G. Baltar, V. Berg, J.-B. Doré, D. Kténas, O. Font-Bach, X. Mestre, M. Payaró, M. Färber, and K. Roth, "The 5G candidate waveform race: a comparison of complexity and performance," *EURASIP Journal on Wireless Communications and Networking*, vol. 2017, no. 1, p. 13, 2017.
- [9] D. Wu, X. Zhang, J. Qiu, L. Gu, Y. Saito, A. Benjebbour, and Y. Kishiyama, "A Field Trial of f-OFDM toward 5G," in *2016 IEEE Globecom Workshops (GC Wkshps)*, Dec 2016, pp. 1–6.
- [10] R. v. Nee and R. Prasad, *OFDM for Wireless Multimedia Communications*, 1st ed. Norwood, MA, USA: Artech House, Inc., 2000.
- [11] V. Vakilian, T. Wild, F. Schaich, S. ten Brink, and J. F. Frigon, "Universal-filtered multi-carrier technique for wireless systems beyond LTE," in *2013 IEEE Globecom Workshops (GC Wkshps)*, Dec 2013, pp. 223–228.
- [12] "FP7 european project - Phydias: physical layer for dynamic spectrum access and cognitive radio, <http://www.phydias-ict.org>."
- [13] G. Fettweis, M. Krondorf, and S. Bittner, "GFDM - Generalized Frequency Division Multiplexing," in *VTC Spring 2009 - IEEE 69th Vehicular Technology Conference*, April 2009, pp. 1–4.
- [14] R. Gerzaguat, D. Demmer, J.-B. Doré, and D. Kténas, "Block-Filtered OFDM: a new promising waveform for multi-service scenarios," in *IEEE ICC 2017 (ICC)*, Paris, France, May 2017. [Online]. Available: <https://www.wong5.fr/wp-content/uploads/2017/04/bf-ofdm-principle.pdf>
- [15] D. Demmer, R. Gerzaguat, J.-B. Doré, D. Le Ruyet, and D. Kténas, "Block-Filtered OFDM: an exhaustive waveform to overcome the stakes of future wireless technologies," in *IEEE ICC 2017 (ICC)*, Paris, France, May 2017.
- [16] E. Arikan, "Channel polarization: A method for constructing capacity-achieving codes for symmetric binary-input memoryless channels," *IEEE Transactions on Information Theory*, vol. 55, no. 7, pp. 3051–3073, July 2009.
- [17] Y. Roth, J.-B. Doré, L. Ros, and V. Berg, "Turbo-FSK: A new uplink scheme for low power wide area networks," in *2015 IEEE 16th International Workshop on Signal Processing Advances in Wireless Communications (SPAWC)*, June 2015, pp. 81–85.
- [18] "Analog device RF agile transceiver AD9361 data sheet," 2017. [Online]. Available: <http://www.analog.com/media/en/technical-documentation/data-sheets/AD9361.pdf>
- [19] "Kathrein antenna, 80010922." [Online]. Available: <http://www.kathrein.fr>
- [20] "Analog Device HMC409LP4, GaAs InGaP HBT 1 W Power Amplifier, 3.3 to 3.8 GHz , url = "http://www.analog.com/media/en/technical-documentation/data-sheets/hmc409.pdf",."
- [21] P. Rosson, D. Dassonville, X. Popon, and S. Mayrargue, "SDR based test bench to evaluate analog cancellation techniques for In-Band Full-Duplex Transceiver," in *Cloud Technologies and Energy Efficiency in Mobile Communication Networks (CLEEN 2017)*, June 2017.
- [22] U. Herzog, A. Georgakopoulos, I. P. Belikaidis, P. Demestichas, S. Diaz, . Carrasco, F. Miatton, K. Moessner, and V. Frascolla, "Quality of service provision and capacity expansion through extended-DSA for 5G," in *2016 European Conference on Networks and Communications (EuCNC)*, June 2016, pp. 200–204.